Mechanical Performance of Oxide/Oxide Ceramic Matrix Composites at elevated temperature

Xuan Gu, Zheng He [a,*], Xiaoyu Sun, JuLiu, Binsheng Wang

College of Aerospace and Civil Engineering, Harbin Engineering University, Harbin 150001 China

[a] sunxiaoyu520634@163.com

Abstract

Tension-compression fatigue behavior of an oxide-oxide ceramic-matrix composite was investigated at 1200 °C in air and in steam. The composite is comprised of an alumina matrix reinforced with Nextel™720 alumina-mullite fibers woven in an eight harness satin weave (8HSW). The composite has no interface between the fiber and matrix, and relies on the porous matrix for flaw tolerance. Tension-compression fatigue behavior was studied for fatigue stresses ranging from 60 to 120 MPa at a frequency of 1.0 Hz. The R ratio (minimum stress to maximum stress) was −1.0. Fatigue run-out was defined as 105 cycles and was achieved at 80 MPa in air and at 70 MPa in steam. Steam reduced fatigue lives by an order of magnitude. Specimens that achieved fatigue run-out were subjected to tensile tests to failure to characterize the retained tensile properties. Specimens subjected to prior fatigue in air retained 100% of their tensile strength. The steam environment severely degraded tensile properties. Tension-compression fatigue was considerably more damaging than tension-tension fatigue. Composite microstructure, as well as damage and failure mechanisms were investigated.

Keywords

Ceramic-matrix composites (CMCs); Oxides; Fatigue; High-temperature properties; Mechanical properties; Fractography.

1. Introduction

Advanced applications such as aircraft turbine engine components, land-based turbines, hypersonic missiles and flight vehicles and, most recently, spacecraft re-entry thermal protection systems have raised the demand for structural materials that exhibit superior long-term mechanical properties and retained properties under high temperature, high pressure, and varying environmental factors. Ceramic-matrix composites (CMCs), capable of maintaining excellent strength and fracture toughness at high temperatures are prime candidate materials for such applications. Because these applications require exposure to oxidizing environments, the thermodynamic stability and oxidation resistance of CMCs are vital issues. The need for environmentally stable composites motivated the development of CMCs based on environmentally stable oxide constituents[1-4].

Efforts to assess the life-limiting behavior of oxide-oxide CMCs under cyclic loading focused mainly on tension-tension fatigue. Yet, in many potential applications, porous-matrix oxide/oxide CMCs may be subjected to fatigue loading with negative ratios of minimum to maximum stress. Therefore a thorough understanding of tension-compression fatigue performance of oxide-oxide CMCs in service environments is critical to their acceptance for high-temperature structural applications. This study investigates the tension-compression fatigue behavior of an oxide-oxide CMC consisting of a porous alumina matrix reinforced with Nextel™720 fibers. Tension-compression fatigue tests were conducted at 1200 °C in air and in steam environments. The composite microstructure, as well as damage and failure mechanisms are discussed.

2. Experimental

The material studied was Nextel™720/alumina (N720/A), an oxide-oxide CMC (manufactured by ATK-COIC, San Diego, CA) consisting of a porous alumina matrix reinforced with Nextel™720 fibers woven in an eight harness satin weave (8HSW). There is no fiber coating. The damage tolerance of the N720/A CMC is enabled by the porous matrix. The composite was supplied in a form of 5.76-mm thick panels comprised of 24 0°/90° woven layers, with a density of ~2.84 g/cm3, a fiber volume of ~44.2%, and matrix porosity of ~22.3%. The fiber fabric was infiltrated with the matrix in a sol-gel process. The laminate was dried with a "vacuum bag" technique under low pressure and low temperature, and then pressureless sintered [5]. The overall microstructure of the CMC is presented in Fig. 1.

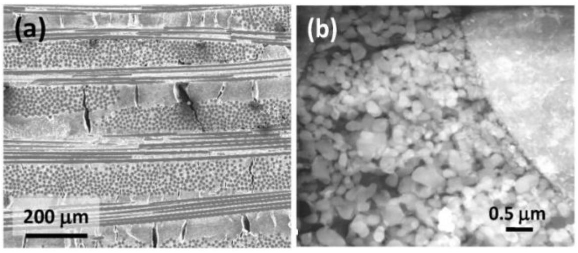

Fig. 1. As-received material: (a) overview, (b) porous nature of the matrix is evident.

Hence the possibility of macroscopic bending during tests due to loss of stiffness with increasing temperature is unlikely. Because compressive loading, and thus the potential for buckling failure modes, was involved in the cycle type, specimens with hourglass-shaped gage section (Fig. 2) were used in all tests. The stress concentration inherent in an hourglass specimen was assessed. Finite element analysis of the specimen shows that the axial stress at the edges in the middle of the hourglass section is only 3.5% higher than the average axial stress.

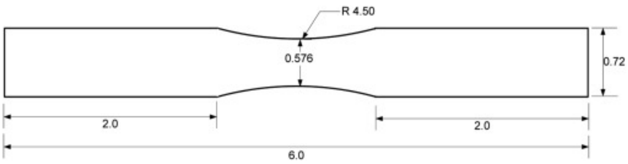

Fig. 2. Test specimen. All dimensions in inches.

Tension-compression fatigue tests were performed in load control with an R ratio (minimum to maximum stress) of −1.0 at 1.0 Hz. Fatigue run-out was defined as 105 cycles. This cycle count represents the number of loading cycles expected in aerospace applications at that temperature. Cyclic stress-strain data were recorded throughout each test, so that modulus change as well as variations in maximum and minimum strains with fatigue cycles and/or time could be examined. All specimens that achieved run-out were tested in tension to failure at 1200 °C in air to determine the retained tensile properties. Fracture surfaces of failed specimens were examined using an optical microscope (Zeiss Discovery V12) and a scanning electron microscope (SEM, Quanta 450).

3. Results and discussion

Results of the tension-compression fatigue tests are shown in Fig. 3 as maximum stress vs. cycles to failure (S–N) curves, where results of the tension-tension fatigue tests from prior work [6] are also included. It is noteworthy that all fatigue failures occurred during the compressive portion of the fatigue cycle.

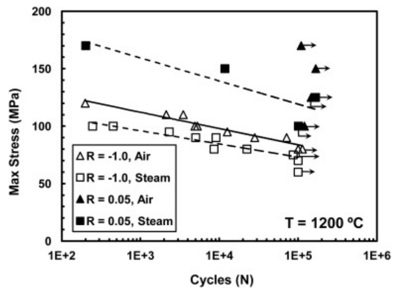

Fig. 3. Fatigue S–N curves for N720/A at 1200 °C in air and in steam. Arrow indicates that failure of specimen did not occur when the test was terminated. Tension-tension fatigue data from Ruggles-Wrenn et al. [6].

Evolution of hysteresis stress-strain response of N720/A composite with cycles at 1200 °C in air and in steam is typified in Fig. 4. It is seen that the hysteresis response produced in tension-compression tests in steam is qualitatively similar to that in air. The hysteresis loops are nearly symmetric about the origin. Such symmetry is maintained for the duration of the test. For each cycle the tensile (compression) modulus was calculated as the slope of the tensile (compressive) portion of the hysteresis loop within the linear region. In all tests, the tensile modulus was approximately the same as the compression modulus for a given cycle. In all tests, the tensile and compressive moduli decrease with fatigue cycling. Progressive decrease in tensile (compressive) modulus is accompanied by an increase in cyclic tensile (compressive) strain. The apparent stiffening observed during compression in Figs. 4a and b is attributed to mechanical impediment of crack closure by matrix debris[7-8].

Fig. 5 shows maximum and minimum strains vs. fatigue cycles for tests conducted at 1200 °C in air and in steam. In all tests performed in this work the evolution of minimum strain with cycles mirrors the evolution of maximum strain. Notably, lower maximum strains were accumulated in tests performed with higher levels of maximum stress. Generally, lower strain accumulation with cycling indicates that less damage has occurred, and that it is mostly limited to some additional matrix cracking. Results in Fig. 5 also reveal that strain accumulation is accelerated in the presence of steam.

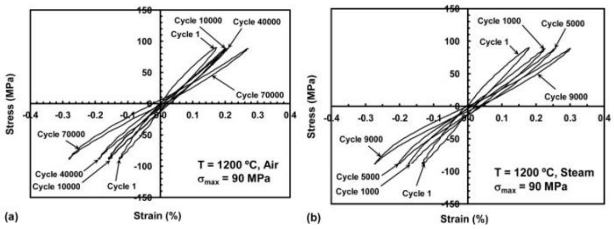

Fig. 4. Typical evolution of stress-strain hysteresis response of N720/A composite with fatigue cycles at 1200 °C (a) in air and (b) in steam. σmax=90 MPa.

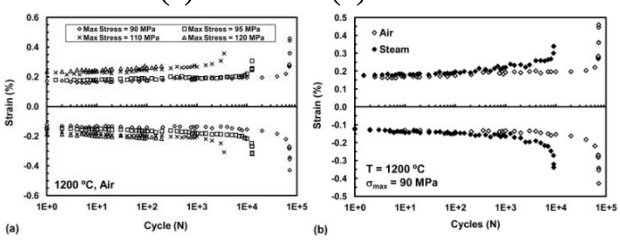

Fig. 5. Maximum and minimum strains vs. fatigue cycles at 1200 °C (a) in air, (b) in air and in steam.

Of importance in cyclic fatigue is the reduction in stiffness (hysteresis modulus determined from the maximum and minimum stress-strain data points during a load cycle), reflecting the damage development during fatigue cycling. The change in normalized modulus (i.e. modulus normalized by the modulus obtained in the first cycle) with fatigue cycles at 1200 °C is shown in Fig. 6. The rate of modulus decay and thus the rate of damage accumulation accelerate slightly with increasing maximum stress. It is noteworthy that although some specimens tested in air achieved fatigue run-out of 105 cycles, a decrease in normalized modulus with cycling was still observed. Decay in normalized modulus is accelerated in the presence of steam, suggesting an increase in the rate of damage accumulation in steam. The degrading effect of steam on the evolution of the normalized modulus is observed for all maximum stress levels. This result is consistent with the decreased number of cycles to failure produced in steam.

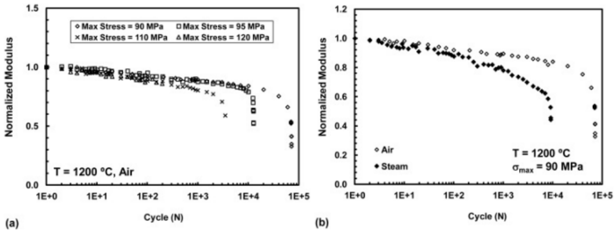

Fig. 6. Normalized tensile modulus vs. fatigue cycles at 1200 °C. (a) in air, (b) in air and in steam.

Retained strength and stiffness of the specimens that achieved fatigue run-out were evaluated in tensile tests performed at 1200 °C (Fig. 7). The specimens subjected to 105cycles of prior tension-compression fatigue with σmax=80 MPa at 1200 °C in air exhibited no loss of tensile strength. However, a modulus loss of 45% was observed. In contrast, prior tension-compression fatigue with σmax of 60 and 70 MPa in steam caused significant degradation of tensile strength. Specimens subjected to 105 fatigue cycles in steam retained only 62–83% of their tensile strength and less than 50% of their modulus. Prior tension-tension fatigue in steam also causes degradation of tensile strength and stiffness[6];[9]. However, the strength and modulus loss were greater in the case of prior tension-compression fatigue.

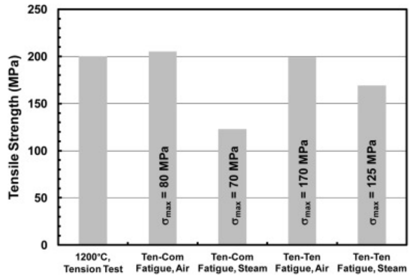

Fig. 7. Retained tensile strength of the N720/A specimens subjected to prior fatigue in laboratory air and in steam environment at 1200 °C. Tension-tension fatigue data from Ruggles-Wrenn et al. [6].

Optical micrographs of fracture surfaces obtained in tension-compression fatigue tests conducted at 1200 °C in air and in steam are shown in Fig. 8. Brushy fracture surfaces and long (~22 mm) damage zones indicative of fibrous fracture are produced in fatigue tests performed with σmax of 100 MPa in air (Fig. 8a) and in steam (Fig. 8b). Not surprisingly, the effects of steam on fracture surface appearance are minimal. These specimens produced the shortest fatigue lives in their respective test environments; hence the 100 MPa fatigue test in steam was of a fairly short duration (<8 min). In contrast, steam has a pronounced effect on the fracture surfaces obtained in tests of longer duration (>24 h). The fracture surface obtained in air with σmax of 80 MPa (Fig. 8c) is similar to that obtained in the fatigue test of a shorter duration performed in air with σmax of 100 MPa (Fig. 8a). Uncorrelated fiber fracture and a fairly long damage zone are still observed. Conversely, the fracture surface of the specimen tested in fatigue with σmax of 75 MPa in steam (Fig. 8d) is dominated by coordinated fiber failure and has a significantly shorter damage zone, suggesting that alumina matrix has densified. The loss of matrix porosity and matrix densification are likely to decrease damage tolerance and degrade composite performance under tensile loading. However, these observations do not explain why tension-compression fatigue is so much more damaging than tension-tension cycling in air as well as in steam.

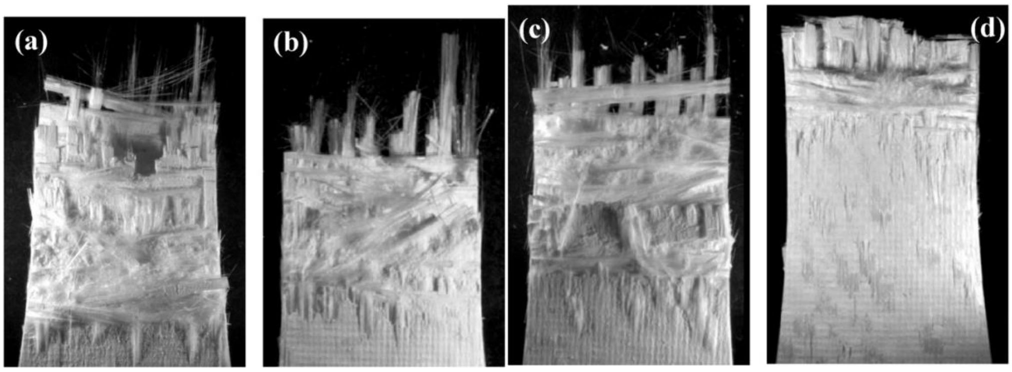

Fig. 8. Fracture surfaces of N720/A specimens tested at 1200° C in tension-compression fatigue: (a) in air, σmax=100 MPa, Nf=4902 cycles, (b) in steam, σmax=100 MPa, Nf=450 cycles, (c)) in air, σmax=80 MPa, Nf=113382 cycles, and (d) in steam, σmax=75 MPa, Nf=86548 cycles.

To gain insight into the mechanisms responsible for drastic reductions in fatigue life seen when compression is included in the load cycle, we examine the fracture surfaces with an SEM The key feature of the fracture surfaces produced in tension-compression fatigue tests in this study is the proliferation of compression curl fiber fractures (Fig. 9). Compression (or cantilever) curl is a telltale feature of flexural fiber fracture. The existence of a compression curl is a sign that the fiber was loaded primarily in bending.

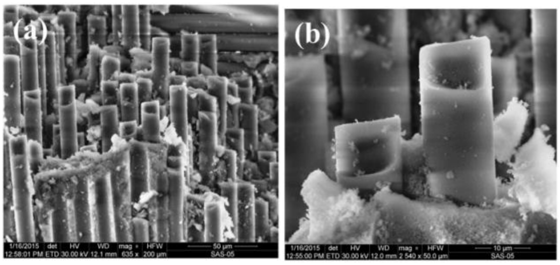

Fig. 9. Fracture surfaces of N720/A specimen tested in tension-compression fatigue at 1200° C. Compression curl fiber fractures.

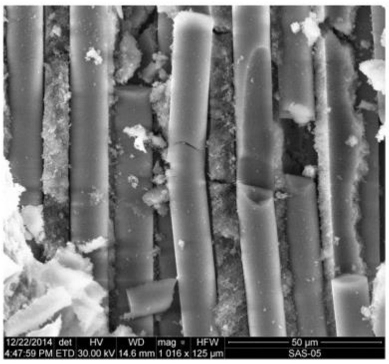

Fig. 10. Fracture surface of N720/A specimen tested in tension-compression fatigue at 1200° C. Fiber micro-buckling.

4. Conclution

The damage and failure of the composite in tension-compression fatigue at 1200 °C in air are due to extensive fiber breakage due to fiber micro-buckling during compression portion of the cycle. The presence of steam causes decomposition of mullite and formation of porous alumina layers on the fiber surfaces, thus decreasing the load-bearing capacity of the N720 fibers. The decomposition of mullite and formation of porous alumina layers are behind the reduced tension-compression fatigue performance of the N720/A composite in steam.

Acknowledgements

This work is supported by the National Natural Science Foundation of China(No. 11602066) and the National Science Foundation of Heilongjiang Province of China (QC2015058 and 42400621-1-15047), the Fundamental Research Funds for the Central Universities.

References

[1] A. Szweda, M.L. Millard, M.G. Harrison, Fiber reinforced ceramic composites member and method for making U.S. patent No. 5, 1997, 601 674.

[2] F.W. Zok Developments in oxide fiber composites J. Am. Ceram. Soc., 89 (2006), pp. 3309–3324

[3] R.J. Kerans, R.S. Hay, T.A. Parthasarathy, M.K. Cinibulk Interface design for oxidation resistant ceramic composites J. Am. Ceram. Soc., 85 (2002), pp. 2599–2632

[4] B. Kanka, H. Schneider Aluminosilicate fiber/Mullite matrix composites with favorable High-temperature properties J. Eur. Ceram. Soc., 20 (2000), pp. 619–623

[5] R.A. Jurf, S.C. Butner Advances in oxide-oxide CMC J. Eng. Gas Turbines Power Trans. ASME, 122 (2000), pp. 202–205

[6] M.B. Ruggles-Wrenn, G. Hetrick, S.S. Baek Effects of frequency and environment on fatigue behavior of An oxide-oxide ceramic composite at 1200 °C Int. J. Fatigue, 30 (2008), pp. 502–516

[7] M. Bouquet, J.M. Birbis, J.M. Quenisset Toughness assessment of ceramic matrix composites Compos. Sci. Technol., 37 (1990), pp. 223–248

[8] G. Camus, L. Guillaumat, S. Baste Development of damage in a 2D woven C/SiC composite under mechanical loading: I. mechanical characterization Compos. Sci. Technol., 56 (1996), pp. 1363–1372

[9] J.M. Mehrman, M.B. Ruggles-Wrenn, S.S. Baek Influence of hold times on the elevated-temperature fatigue behavior of An oxide-oxide ceramic composite in air and in steam Compos. Sci. Technol., 67 (2007), pp. 1425–1438